ACS APPLIED MATERIALS & INTERFACES

Research Article

www.acsami.org

Graphene Oxide–Rare Earth Metal–Organic Framework Composites for the Selective Isolation of Hemoglobin

Jia-Wei Liu,[†] Yue Zhang,[†] Xu-Wei Chen,*[,†] and Jian-Hua Wang*[,†,‡]

[†]Research Center for Analytical Sciences, College of Sciences, Northeastern University, Shenyang 110819, China

[‡]Collaborative Innovation Center of Chemical Science and Engineering, Tianjin 300071, China

Supporting Information

ABSTRACT: Graphene oxide-La(BTC)$(H_2O)_6$ (H_3BTC=1,3,5-benzenetricarboxylic acid) metal organic framework composites (LaMOF-GO$_n$, n = 1–6, corresponding to the percentage of GO at 1, 2, 3, 4, 5, and 10%) are prepared through a simple and large-scale method at room temperature. The obtained composites are characterized by ATR-FTIR spectra, SEM, XRD, TGA, and N_2 adsorption–desorption isotherm. The presence of GO significantly changes the morphologies of the composites from spindly rectangular rods to irregular thick blocks and increases their surface area from 14.8 cm^2 g^{-1} (LaMOFs) to 26.6 cm^2 g^{-1} (LaMOF-GO$_3$), whereas at the same time, the crystalline structure of La(BTC)$(H_2O)_6$ is maintained. As a novel solid-phase adsorbent the LaMOF-GO composite exhibits outstanding adsorption properties for proteins. The strong hydrophobic interaction, especially π–π interaction between protein and the composite, is the main driving force for protein adsorption. In particular, highly selective isolation of hemoglobin (Hb) is achieved by using LaMOF-GO$_3$ composite as sorbent in 4 mM B-R buffer containing 0.05 mol L^{-1} NaCl at pH 8. The retained Hb could be effectively recovered with a 1 mM B-R buffer at pH 10, giving rise to a recovery of 63%. The practical applicability of the LaMOF-GO$_3$ composite is demonstrated by the selective adsorption of Hb from human whole blood, and SDS-PAGE assays indicate that Hb could be selectively isolated with high purity from biological samples of complex matrixes.

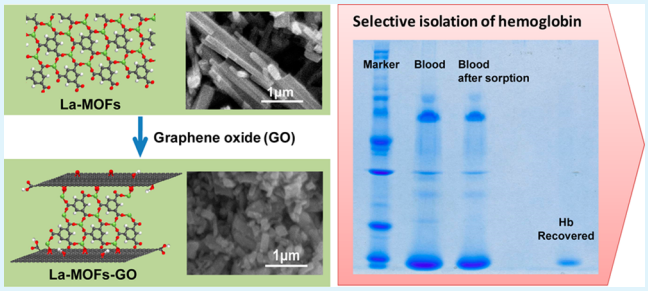

KEYWORDS: *graphene oxide, metal–organic frameworks, lanthanum, composite, hemoglobin, isolation*

INTRODUCTION

During the past decade, graphene has attracted great attention in both experimental and theoretical scientific communities. Becuase of the specific and outstanding structural, electronic, mechanical, and thermal properties,[1] graphene and its derivatives have been employed as novel carbon nanomaterials in various fields, e.g., electronic devices, energy storage, chemical and electrochemical sensors, catalysis, as well as biological and biomedicine applications.[2−7] For bioseparation, graphene and its oxidized derivative, i.e., graphene oxide (GO), exhibits favorable biocompatibility and high adsorption capacity toward proteins and peptides[8−10] because of its huge specific surface area and abundant binding sites on the surface. Nevertheless, graphene/GO generally exhibits nonspecific adsorption of protein species and the poor recovery of the adsorbed proteins from the surface of graphene/GO makes their use limited from the practical point of view. Therefore, in practice, graphene/GO usually combines with organic molecules[11] or inorganic materials[9,12−14] through covalent or noncovalent functionalization processes, forming hybrids/nanocomposites as sorbents for the separation of biomolecules. The graphene/GO-based composites not only maintain the unique properties of graphene/GO, but also effectively overcome its intrinsic shortcomings, which facilitates their applications in the field of biological separation.

Metal–organic frameworks (MOFs) are novel inorganic–organic hybrid materials and have aroused great interests in recent years. MOFs are composed of metal clusters and organic linkers to form infinite crystalline lattices through self-assembly.[15−17] The unique properties of MOFs, including permanent nanoscale porosity, high surface area, uniform but tunable pore size, in-pore functionality, and out-surface modification,[18] make MOFs as an excellent candidate for the applications of gas storage,[19] catalysis,[20] gas sensor,[21] and separation.[22] For the purpose of sample preparation, MOFs exhibit enormous advantages and potential applications. MOF-5 has been employed as sorbent for in-field sampling and preconcentration of atmospheric formaldehyde giving rise to much improved concentration effect over Tenax TA and Carbograph 1TD.[23] A lot of efforts were directed to the preparation of graphene/GO-MOFs composites to combine the unique properties of both graphene/GO layers and MOFs for various applications. MOF-5-GO composites prepared

Received: March 13, 2014
Accepted: June 20, 2014
Published: June 20, 2014

through solvothermal process illustrated that MOF-5 blocks attach on GO through the replacement of oxygen atoms in ZnO_4 tetrahedra by epoxy groups on the surface of GO,[24] giving rise to variation of the structures and morphologies of MOF-5. A structure-directing template by using benzoic acid-functionalized graphene (BFG) nanosheets was found to affect the crystal growth of MOF-5 and an unusual MOF/BFG nanowire was derived.[25] The graphene showed template-directed nucleation effect on the structural motifs of MOFs and the intercalation of graphene in MOF facilitated new electrical properties in the otherwise insulating MOF. The graphene/GO-MOFs composites have also been applied to catalysis, gas removal, and optical sensing.[26−28] The graphene/GO-based MOFs composites provided a powerful strategy for developing new materials and broadened their applications in various fields. However, to the best of our knowledge, there is so far no report on the application of graphene/GO-MOFs composites to the adsorption and separation of proteins.

Herein, we report a novel graphene oxide−$La(BTC)(H_2O)_6$ metal−organic framework (LaMOF-GO) composite. This composite material is for the first time used for the purpose of protein adsorption. The LaMOF-GO composite exhibits favorable selectivity for the adsorption of protein, in this particular case, hemoglobin. High purity hemoglobin is obtained which is suitable for further biological studies. The results of this work open a new avenue for the development of biomaterials or biosorbents for the purpose of isolation/separation of biomacromolecules from complex sample matrixes.

EXPERIMENTAL SECTION

Materials and Reagents. High-purity graphite powder (spectral grade), lanthanum nitrate hydrate ($La(NO_3)_3{\cdot}6H_2O$) and *N*,*N*-dimethylformamide (DMF) are purchased from Sinopharm Chemical Reagent Co. Ltd. (Shanghai, China). 1,3,5-benzenetricarboxylic acid (H_3BTC, >98%) is acquired from TCI (Tokyo Kasei Kogyo Co. Ltd., Japan). Potassium permanganate, sulfuric acid (98%, w/w), sodium nitrate, sodium hydroxide, hydrogen peroxide (30%, w/w), acetic acid, phosphoric acid, and boric acid are obtained from Bodi Chemical Holding Co. Ltd. (Tianjin, China). All these chemicals are at least of analytical reagent grade and are used as-received without further purification. Eighteen MΩ cm deionized water is used throughout.

Hemoglobin (Hb, H2625, 95%) and bovine serum albumin (BSA, A1933, ≥98%) are obtained from Sigma-Aldrich (St. Louis, USA) and used as received. The protein molecular weight marker (broad, 3452, Takara Biotechnology Company, Dalian, China) is a mixture of nine purified proteins (M_r in kDa: myosin, 200; β-galactosidase, 116; phosphorylase B, 97.2; serum albumin, 66.4; ovalbumin, 44.3; carbonic anhydrase, 29; trypsin inhibitor, 20.1; lysozyme, 14.3; aprotinin, 6.5).

Britton-Robinson (B-R) buffers are employed for the investigations of protein adsorption behaviors. Typically, 4 mM acetic acid, phosphoric acid, and boric acid are mixed together and the pH values are adjusted by 0.2 mol L^{-1} NaOH. The protein stock solutions (1.0 mg mL^{-1}) are prepared by dissolving certain amount of proteins in buffers and the working solutions are obtained by stepwise dilution of the stock solutions with corresponding buffers. The eluent or stripping solution is prepared by diluting the B-R buffer appropriately and adjusting to pH 10.

Preparation of the LaMOF-GO Composites. Preparation of GO based on the modified Hummers' method.[29,30] Briefly, 5.0 g of graphite powder is pretreated by mixing with concentrated H_2SO_4 (15 mL), potassium persulfate (5.0 g), and phosphorus pentoxide (5.0 g) and heating at 80 °C for 6 h under continuous stirring. After diluted with 100 mL deionized water, the product is centrifuged, washed by water until neutral and dried at 60 °C under vacuum for overnight. The preoxidized graphite (4.0 g) is mixed with concentrated H_2SO_4 (136 mL) in an ice bath at 0 °C, followed by successively adding 3.2 g of $NaNO_3$ and 18 g of $KMnO_4$ into the above dispersion with vigorous mechanical stirring to keep the temperature below 20 °C. Afterward, the mixture is stirred at 35 °C for 2 h, and then continuously stirred at room temperature for 7 days. The viscous brown product is transferred into 500 mL glass beaker and H_2O_2 (3%, v/v) solution is drop-wisely added until the mixture becomes bright yellow. The suspension is separated by centrifugation at 10 000 rpm for 10 min, washed by HCl (1:10, v/v) and deionized water successively until the impurity is completely stripped off and a neutral supernatant is obtained. Finally, graphite oxide is collected and dried under vacuum at 60 °C for 24 h.

Synthesis of $La(BTC)(H_2O)_6$: lanthanum metal−organic frameworks (LaMOFs) are prepared by following a literature method with modifications.[31,32] Typically, 162.5 mg $La(NO_3)_3$ (ca. 0.5 mmol) is dissolved in 15 mL of water under magnetic stirring and 15 mL of DMF containing H_3BTC (0.5 mmol, 105.1 mg) is added into the above solution subsequently. After vigorous stirring at room temperature for 6 h, the supernatant is removed and a white precipitate is obtained by centrifuging at 10 000 rpm for 5 min. The product is then washed by deionized water for three times and dried in an oven at 90 °C under vacuum overnight. The elemental analysis results for the obtained product (C, 23.93%; H, 3.09%; O, 44.36%) are consistent with those of the calculated results for $C_9H_{15}LaO_{12}$ (C, 23.80%; H, 3.33%; O, 42.28%).

Preparation of the LaMOF−GO composites: GO is well-dispersed in water by mild sonication for 2 h to obtain a yellow-brown aqueous suspension (1.0 mg mL^{-1}). The LaMOF-GO composites are prepared through a similar procedure as the synthesis of LaMOFs. In a typical reaction, 162.5 mg of $La(NO_3)_3$ (ca. 0.5 mmol) is dissolved in 6.7 mL of water and 8.3 mL of GO suspension (8.3 mg) is added under magnetic stirring. The mixture is then continuously stirred at room temperature for 4 h to achieve complete ion-exchange of La^{3+} with oxygen functional groups on the surface of GO (e.g., carboxyl, hydroxyl and epoxide groups). Afterward, 105.1 mg of H_3BTC (0.5 mmol) dissolved in 15 mL of DMF is added into the above solution. The reaction is taking place with strong magnetic stirring for 6 h and a gray precipitate is obtained after centrifugation at 10 000 rpm for 5 min. The product is washed by deionized water for three times and dried at 90 °C under vacuum. The composites with various GO ratios of 1, 2, 3, 4, 5, and 10% are prepared by following the same process with different volumes of GO solution. The products are referred as LaMOF-GO_n (n = 1−6). In fact, with the increase in GO ratio, the high concentration of GO in permanent aqueous solution (>2 mg mL^{-1}) might be adverse to the dispersion of GO, and thus cause deterioration on the formation of LaMOF-GO composite. Therefore, in practice, the largest GO ratio reaches 10%. In the present study, the GO ratio is calculated based on the starting mass of the materials involved in the preparation of the LaMOF-GO composite, as illustrated in the following

$$\text{GO ratio\%} = \text{GO mass/total mass}(La(NO_3)_3,\ H_3BTC, \text{and GO})$$

Characterizations. Attenuated total reflection Fourier Transform Infrared (ATR-FTIR) spectroscopy is employed to confirm the formation of LaMOF-GO composites by using Nicolet-6700 FT-IR spectrophotometer (Thermo Fisher Scientific, USA) from 650 to 4000 cm^{-1} with ZnSe crystal. The morphology variations of LaMOF-GO_n composites are recorded by S-3400N scanning electronic microscopy (SEM, Hitachi High Technologies, Japan). X-ray diffraction (XRD) patterns are recorded on an X′ Pert Pro MPD X-ray diffractometer (PW 3040/60, PANalytical B. V., Holland) with Cu−Kα irradiation (λ = 1.5406 Å) in the range of 2θ from 5 to 60°. The thermogravimetric analysis (TGA) is measured by a TGA/DSC 1 STAR^e System (Mettler-Toledo, Switzerland) from 25 to 800 °C with a heating rate of 10 °C min^{-1} under N_2 atmosphere. The nitrogen adsorption−desorption isotherms are obtained at −196 °C by using a BK224T-12 Instrument (Beijing JWGB Sci.&Tech. Co., Ltd., China). Prior to the measurements, the three composites, i.e., LaMOFs, LaMOF-GO_3, and LaMOF-GO_6, are degassed at 100 °C under vacuum for 10 h. The elemental content of C, H, and O in LaMOFs are measured by use of a

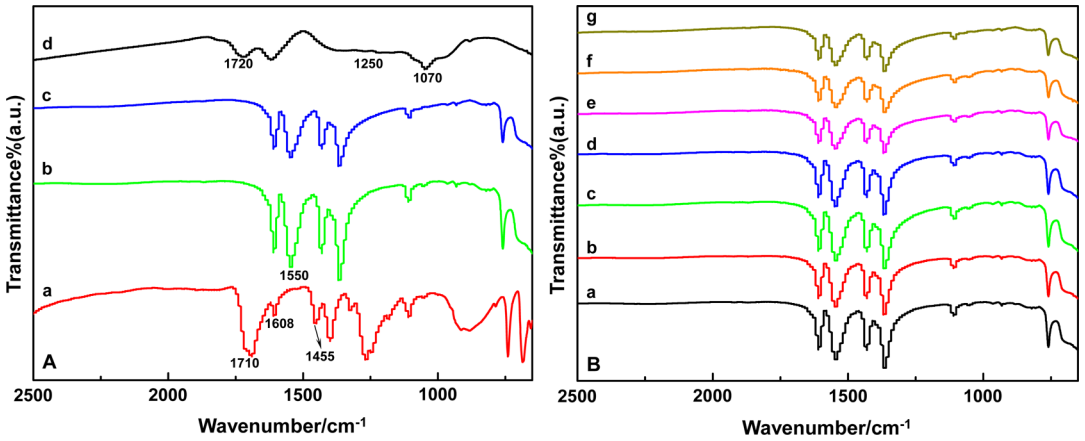

Figure 1. (A) ATR-FTIR spectra of (a) H_3BTC ligands, (b) LaMOFs, (c) LaMOF-GO_6, and (d) GO; (B) ATR-FTIR spectra of (a) LaMOFs and (b–g) LaMOF-GO_n composites with various percentage of GO (1, 2, 3, 4, 5, and 10%, respectively).

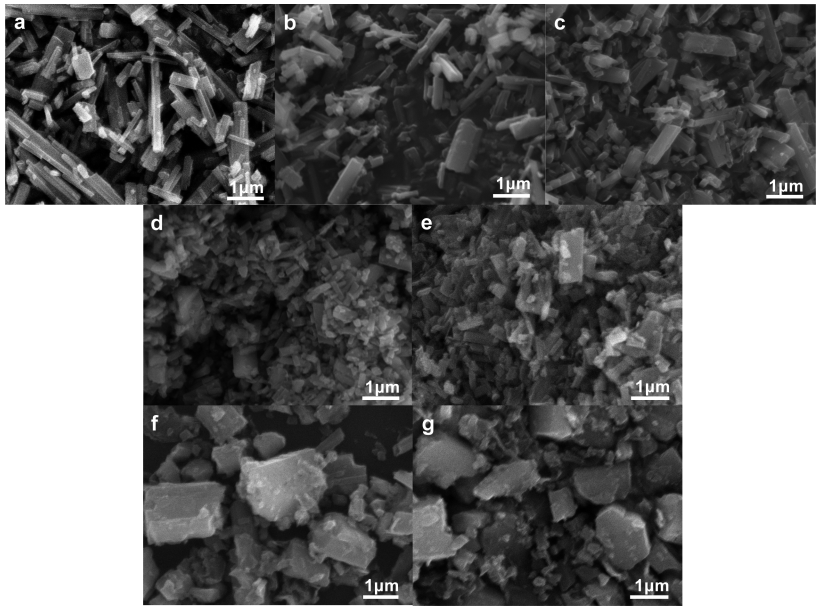

Figure 2. SEM images of (a) LaMOFs and (b–g) LaMOF-GO_n composites (n = 1–6, respectively).

Vario EL III Elemental Analyzer (Elementar Analysensysteme GmbH, Germany).

Adsorption of Proteins with the LaMOF-GO Composites. In the present work, Hb (pI 6.8–7.0) and BSA (pI 4.9) are employed as the model proteins. First, the adsorption behaviors of the two proteins on the three composites, i.e., LaMOFs, LaMOF-GO_3 and LaMOF-GO_6, are investigated within a range of pH 2–11. Generally, the LaMOF-GO composites are dispersed in water by mild sonication to form a homogeneous solution (10 mg mL^{-1}). Fifty microliters of LaMOF-GO composites suspension is transferred into a 2.0 mL plastic tube and centrifuged at 12000 rpm to remove the supernatant. Then a protein solution (50 mg L^{-1}, 1.0 mL) is added and the mixture is shaken vigorously for 30 min to facilitate the adsorption of proteins onto the surface of composites. When the adsorption process is completed, the mixture is centrifuged at 10000 rpm and the supernatant is collected to quantify the residual proteins left in the original solution by use of an U3900 UV–vis Spectrophotometer (Hitachi High Technologies, Japan).

The proteins adsorbed onto the LaMOF-GO_3 composites are effectively recovered with B-R buffer (1.0 mM, pH 10.0). Typically, 1.0 mL of eluent is mixed with the composites and continuously oscillated for 30 min to facilitate the elution/desorption of the adsorbed proteins from the surface of the LaMOF-GO_3 composite. The supernatant with recovered protein species is collected by centrifugation at 10 000 rpm for 5 min for the ensuing investigations.

Isolation of Hemoglobin from Human Whole Blood. The practical applicability of the LaMOF-GO_3 composite is demonstrated by performing the selective isolation of hemoglobin from human whole blood. In practice, human whole blood (obtained from the Hospital of Northeastern University donated by healthy volunteer and stored at −20 °C) is 100-fold diluted with 0.004 mol L^{-1} B-R buffer solution containing 0.05 mol L^{-1} NaCl at pH 8. After shaking and centrifugation, the cell debris is removed and the supernatant is collected for the isolation process as described in previous section. After the adsorption process, the surface of LaMOF-GO_3 composite is prewashed by water to eliminate the loosely retained interfering components. The adsorbed Hb is then recovered by 1 mM B-R buffer at pH 10 and the collected protein is further analyzed by SDS-PAGE. The SDS-PAGE assay is performed by using 12% polyacrylamide resolving gel and 5% polyacrylamide stacking gel with standard discontinuous buffer systems.

RESULTS AND DISCUSSION

Characterizations of the LaMOF-GO_n Composites. The formation of LaMOFs and LaMOF-GO_n composites are confirmed by ATR-FTIR spectra. As shown in Figure 1A, the

absorption band of C=O related to carboxyl groups at 1710 cm^{-1} and two characteristic bands at 1608 and 1455 cm^{-1} corresponding to the stretching vibrations of phenyl rings are observed in the spectrum of H_3BTC ligands (a).[31] After the formation of LaMOFs, the adsorption band at 1710 cm^{-1} disappears while a new band at 1550 cm^{-1} assigned to the stretching vibrations of COO^- groups is observed, which demonstrates the full deprotonation of H_3BTC ligands and the conversion of carboxyl into carboxylate moieties (b).[31] In the spectrum of LaMOF-GO_6 (c), no obvious difference is observed in comparison with that of LaMOFs. The characteristic absorption bands of oxygen-containing groups of GO, e.g., carboxyl, epoxide and hydroxyl groups at 1720, 1250, and 1070 cm^{-1} (as shown in d),[33] are not seen in the spectrum attributed to the fact that they have coordinated with La^{3+} cations. It is evident that GO participates in the formation of LaMOFs crystals through capturing La^{3+} cations with the oxygen-containing groups on its surface. Besides, the similar FT-IR spectra of LaMOFs and LaMOF-GO_6 composites show that the structure of LaMOFs crystals is well-maintained even in the presence of large amount of GO.

For further investigating the effect of GO on the structure of LaMOFs crystals, FT-IR spectra of LaMOF-GO_n composites with various amount of GO (at 0−10%) are recorded (Figure 1B). It is seen that all the composites exhibit identical absorption bands as those in LaMOFs, suggesting that they own same coordination structure.[34] This result further indicates that GO acts as just a template to fasten the La^{3+} cations and facilitate the growth of $La(BTC)(H_2O)_6$ crystals on its surface, without destruction of the coordination structure of the crystals.

It is known that graphene oxide or functional graphene nanosheets could interfere the crystallization of MOFs and significantly change their surface morphologies during the synthesis procedure of MOFs.[24,25] In this work, the changes of surface morphologies of LaMOFs and LaMOF-GO_n composites are recorded by SEM images. As illustrated in Figure 2, the LaMOFs are spindly rectangular rods with a width of 150−300 nm and a length of a few micrometers (Figure 2a). In the presence of GO, significant changes were observed for the surface morphologies of LaMOF-GO_n composites, especially with increasing amounts of GO (Figure 2b-g). When the amount of GO is lower than 5%, the LaMOF-GO_n (n = 1−4) composites keep the shape of rectangular bars as LaMOFs, whereas their lengths become shorter with the increase of the amount of GO (Figure 2b−e). In contrast, LaMOF-GO_n composites (n = 5−6) at high percentage of GO (5−10%) become irregular and thick blocks with larger diameter, which is quite different in comparison with the above composites (Figure 2f, g). The formation mechanism of LaMOF-GO composites is illustrated in Figure 3. For LaMOFs, the center La atom is nine coordinated by six oxygen atoms from water molecules as well as three oxygen atoms from three carboxylate groups of H_3BTC ligands.[35] The spindly rectangular structure of LaMOFs is ascribed to the extending of parallel 1D ribbon-like molecular motifs along one axis and stacking through phenyl groups of BTC^{3-} ligands superimposition along another axis (Figure 3a).[35] When GO is added, the La^{3+} cations first coordinate with the oxygen-containing groups (carboxyl, hydroxyl and epoxide groups) on the surface of GO to form the GO-La complex. Then the fastened and free La^{3+} cations capture H_3BTC ligands to form LaMOFs crystals on the surface of GO. Due to the formation of GO-La complex, the amount of free La^{3+} cations in the solution decreases so that the length of LaMOFs crystals is limited. Moreover, the GO-La complex also acts as a terminator to interrupt the growth of crystals, which makes the LaMOF-GO composites short (Figure 3b). With the increase of percentage of GO (<5%), less free La^{3+} cations are left and higher frequent interruptions take place so that the length of LaMOF-GO rods become shorter. However, when the amount of GO is even higher (>5%), apart from much more La^{3+} cations are fastened onto the GO surface, the LaMOFs crystals are formed between GO-La complex layers simultaneously, resulting in the formation of irregular and thick blocks (Figure 3c). Considering the similarity of these composites, three typical materials, i.e., LaMOFs, LaMOF-GO_3, and LaMOF-GO_6, are selected as models for the following investigations.

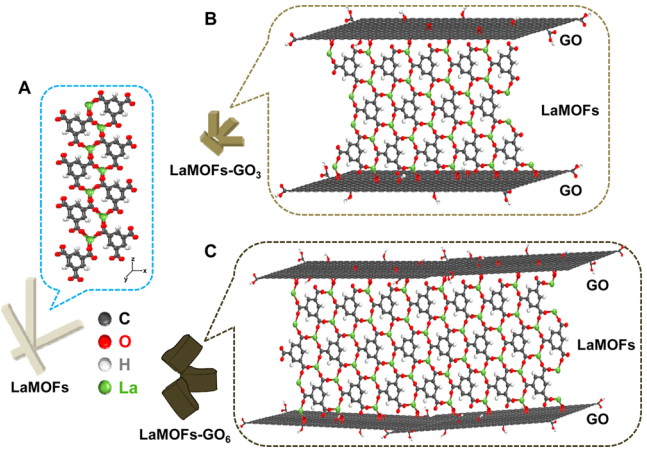

Figure 3. Formation mechanism of (A) LaMOFs, (B) LaMOF-GO composites with GO percentage <5%, and (C) LaMOF-GO composites with GO percentage >5%, the six water molecules coordinated with the La^{3+} cation are not shown.

The XRD patterns of simulated LaMOFs, the prepared LaMOF, LaMOF-GO_3, and LaMOF-GO_6 composites are illustrated in Figure 4. The diffraction patterns of the prepared LaMOFs exhibit sharp and narrow peaks demonstrating that the product is high-quality crystalline (Figure 4b). All the XRD peaks can be indexed to the known bulk phase of La(BTC)-

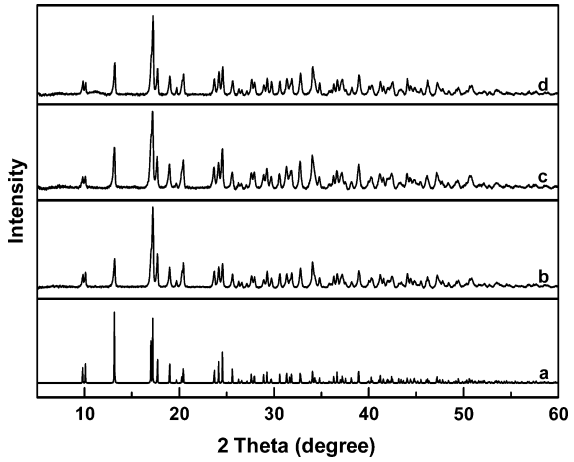

Figure 4. XRD patterns of (a) the simulated LaMOFs, (b) the as-prepared LaMOFs, (c) the LaMOF-GO_3 composite, and (d) the LaMOF-GO_6 composite.

$(H_2O)_6$ (CCDC 290771),[35] indicating that the crystal structure of the obtained product can be inferred to be monoclinic space group *Cc*.[32] The similar XRD patterns for the prepared and the simulated LaMOFs (Figure 4a) as well as the others reported elsewhere[31−33] demonstrate that they have the same crystal structure in spite of being prepared under different reaction conditions. In addition, the presence of different amount of GO gives rise to almost identical XRD patterns for LaMOF-GO_3 and LaMOF-GO_6 composites with that of the prepared LaMOFs and no impurity peaks are recorded. This implies that the presence of GO does not destroy the crystal structure and the crystalline composites are isostructural to La(BTC)-$(H_2O)_6$[31] (Figure 4c, d). This observation is in agreement with the results of ATR-FTIR spectra.

The thermal properties of LaMOFs and LaMOF-GO composites are investigated by use of thermogravimetric analysis (TGA) and the results are shown in Figure S1 in the Supporting Information. Pure LaMOFs exhibits two significant mass losses at ca. 150 and 550 °C, respectively. The first mass loss of ca. 23.1% taken place at around 150 °C is derived from the dehydration process of LaMOFs and a dehydrated material with a formula La(BTC) is obtained. Then this phase is stable until the decomposition of coordination polymer occurs at about 550 °C and a 29.9% mass loss is obtained due to the pyrolysis of BTC^{3-} ligands. The final residue may be the lanthanum oxide as confirmed by XRD patterns.[31] For the TG curves of LaMOF-GO_3 and LaMOF-GO_6 composites, apart from the thermal decomposition of La(BTC)$(H_2O)_6$ as observed for LaMOFs, further mass losses at 50−250 °C are obtained because of the decomposition of GO. GO usually loses water molecules at below 100 °C as well as the oxygen-containing groups at ca. 150−200 °C.[11] In addition, a significant increase of mass loss is observed with the increase of amount of GO from 3 to 10%. The TG results suggest that there is no specific strong bonding force between GO and LaMOFs crystal and both of them keep their respective structure and thermal properties in the composites.

Figure 5 illustrates the nitrogen adsorption−desorption isotherms of LaMOFs, LaMOF-GO_3 and LaMOF-GO_6 composites. Unlike the typical classification of IUPAC, the isotherm of LaMOFs appears to show normal Type II adsorption with a Type H3 hysteresis loop at high relative pressure, which is termed pseudo Type II isotherm (Figure 5a).[36] The porosity of LaMOFs is obtained by the BJH (Barrett−Joyner−Halenda) method of mesopore analysis with adsorption branch (see Figure S2a in the Supporting Information) and the result shows a broad distribution of pore width between 2 and 200 nm. However, these mesopores and macropores cannot represent the intrinsic property of the structure of LaMOFs, in contrast, they are probably derived from the structural defects and voids between the crystals.[36] In the presence of GO, the isotherms of LaMOF-GO_3 and LaMOF-GO_6 composites still belong to pseudo Type II with evident Type H3 hysteresis loops, suggesting their similar N_2 adsorption−desorption behavior with LaMOFs (Figure 5b, c). It is noticeable that a properly large hysteresis appears in the capillary condensation range and the distributions of pore width are broadened to a range of 2−2000 nm (see Figure S2b, c in the Supporting Information). In fact, the obvious hysteresis loops are attributed to the assemblages of platelike particles, i.e., LaMOF-GO composites in this case.[36] It is known that GO displays as two-dimensional thin layers and plays as a template and terminator in the growth of LaMOFs crystals, therefore the platy aggregates between intra- and inter-LaMOF-GO units lead to plenty of mesopores and macropores within a wide range of pore diameters. Account for the formation of more platy aggregates with the increase of GO amount from 3 to 10%, a broadened hysteresis loop is clearly observed.

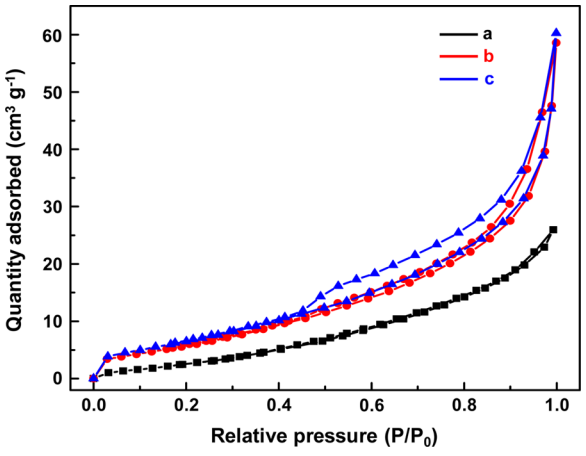

Figure 5. Nitrogen adsorption−desorption isotherm of (a) LaMOFs, (b) LaMOF-GO_3 composite, and (c) LaMOF-GO_6 composite.

The surface areas of the three composites are calculated under BET (Brunauer−Emmett−Teller) method by using the adsorption data in the range of P/P_0 from 0.05 to 0.35 and the results are illustrated in Table S1 (see the Supporting Information). The surface area of LaMOFs is fairly low because there is no micropore formed under the preparation condition and the nitrogen adsorption is only performed on its surface. While with the participation of GO in the growth of LaMOFs crystals, the surface area of LaMOF-GO_3 increases almost twice comparing with that of LaMOFs, i.e., from 14.8 to 26.6 $cm^2\ g^{-1}$. It is reasonable that the decrease of size of LaMOFs rods induced by GO layers lead to the increase of surface area. As the amount of GO reaches 10%, a slight decrease of surface area of LaMOF-GO_6 is obtained due to the irregular blocks with large size (Figure 2g). It should be noted that the surface areas for LaMOFs and LaMOF-GO are obviously smaller than those for regular MOFs; however, in the present case, they are large enough for the adsorption of proteins in biological samples.

Adsorption of Proteins by the LaMOF-GO Composites. The protein adsorption behaviors of the LaMOF-GO composite have been compared with those by LaMOFs and GO themselves. For this purpose, the three composites, i.e., LaMOF, LaMOF-GO_3 and LaMOF-GO_6, are employed as sorbents for the adsorption of protein species, BSA and Hb in the present case. Figure 6 shows the adsorption performances of the two proteins on the three sorbents at various pHs. It is clearly seen that BSA and Hb exhibit similar adsorption behaviors on these sorbents. The maximum adsorptions are achieved at pHs close to their ioselectric points (pI), i.e., at pH 5.0 for BSA (pI 4.9) and pH 7.0 for Hb (pI 6.8−7.0), respectively. These observations indicate that the strong hydrophobic interactions between protein species and the surface of the composites might be the main driving force for the adsorption of proteins onto the composites.[9,37] Actually, the structure of LaMOFs is constructed by the coordination of La^{3+} cations with phenyl-rich ligands, which could provide considerable $\pi-\pi$ interactions between the amino acid residues of proteins and the surface of LaMOFs. On the other hand, the

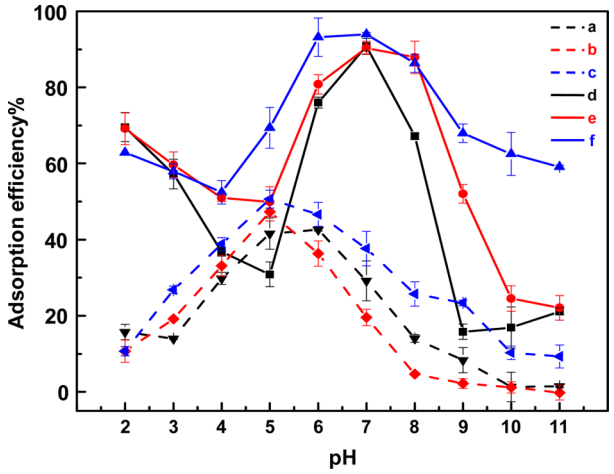

Figure 6. pH dependence of the adsorption efficiencies of protein species onto the three composite materials: LaMOFs toward (a) BSA and (d) Hb; LaMOF-GO_3 composite toward (b) BSA and (e) Hb; LaMOF-GO_6 composite toward (c) BSA and (f) Hb. The concentration and volume of Hb solution, 50 mg L^{-1} and 1.0 mL; the amount of the composite materials, 0.5 mg; the adsorption time, 30 min.

large area of conjugate π-electron moieties in the GO structure provides an alternative contribution to the protein adsorption. As is widely recognized that proteins are uncharged at around their ioselectric points and more hydrophobic residues usually embedded inside the hydrophobic interior, e.g., porphyrin rings of Hb and/or tryptophan/tyrosine residues of proteins. The proteins are prone to expose to the surface of the composites, and thus facilitates their adsorption. This has been demonstrated by our previous studies.[9] Therefore, at a pH around the pI values of proteins, the strongest $\pi-\pi$ interactions lead to the most effective adsorption of proteins onto the surface of the composites.

It is interesting that the obvious different adsorption efficiencies of Hb and BSA are obtained within a wide pH range. This reveals a discriminatory $\pi-\pi$ interaction of Hb and BSA with the sorbents, and thus provides selectivity toward the adsorption of Hb. Hemoglobin is a typical globular protein whose tetramer contains four ferrohemes inside the hydrophobic interiors.[38] At a pH close to the pI of Hb, the strong face-to-face $\pi-\pi$ interactions between heme moieties and the surface of the composites could significantly facilitate the adsorption of Hb.[9] However, there are no heme groups in the structure of BSA, thus $\pi-\pi$ interactions between BSA and the composites are much weak which leads to a low adsorption efficiency. On the other hand, a high adsorption efficiency of Hb onto the sorbents is achieved in acidic medium at pH 2−3. This is an indication of other binding force between the proteins and the composites. It is the fact that the pK_a value of H_3BTC is 3.12,[39] which implies that the carboxylate groups of BTC^{3-} ligands could get reprotonated in a strong acidic medium. This might cause the destruction of the coordination bonds between La^{3+} cations and BTC^{3-} ligands, especially those on the surface of the crystals and thus some La^{3+} cations own free coordination positions. In addition, La^{3+} cations exhibit high metal affinity with hemoglobin through coordination force.[40] Therefore, those La^{3+} cations with free coordination positions could strongly coordinate with Hb molecules and result in high adsorption efficiency at a low pH value.

In comparison with the LaMOFs, the presence of GO improves the adsorption efficiencies of proteins in a wide pH range, particularly at a higher percentage of GO (Figure 6b, c for BSA and e, f for Hb). It is remarkable that GO also exhibits high selectivity for separation of Hb, and the strong $\pi-\pi$ interactions between GO nanosheets and Hb are the main driving force.[9] Herein, the similar adsorption properties of LaMOFs and GO provide synergistic effect on the protein adsorption. In particular, when using LaMOF-GO_3 composite as sorbent, a high adsorption efficiency of ca. 88% for Hb is achieved at pH 8.0 where virtually no adsorption of BSA is observed. These different adsorption behaviors for the two protein species provide a promising potential for the development of a novel selective isolation protocol with LaMOF-GO_3 composite as sorbent. With the presence of 3% GO not only increases the surface area of LaMOF-GO_3 composite to facilitate a high sorption capacity, but also improves the selectivity toward the two model proteins.

Adsorption of Hb onto LaMOF-GO_3. On the basis of the previous discussions, LaMOF-GO_3 composite displays favorable selectivity for the adsorption of Hb based on the strong $\pi-\pi$ interactions between Hb molecules and the LaMOF-GO_3 composite. Therefore, a novel solid-phase extraction protocol for the isolation of Hb from complex sample matrix is developed. The important experimental parameters affecting the adsorption and desorption of hemoglobin are further evaluated.

As discussed previously, the adsorption of hemoglobin is favorably performed at pH 8. According to the adsorption mechanism, the $\pi-\pi$ interactions between Hb and the composites could be strengthened by increasing the ionic strength of the sample solution and an increase of adsorption capacity could be obtained. As illustrated in Figure S3 (see the Supporting Information), when adding a certain amount of NaCl into the sample solutions (0.0−1.0 mol L^{-1}), the adsorption efficiency of Hb is increased to ca. 90% at a NaCl concentration of 0.05 mol L^{-1} and afterward a slight decrease of the adsorption efficiency is encountered by further increase of NaCl concentration. The increase of adsorption efficiency is attributed to the removal of water molecules around protein structures by salt which facilitates the exposure of hydrophobic residues in Hb framework onto the surface of the composites, whereas the decrease of adsorption might be explained by the competition of NaCl on the composite surface.[9] In practice, a NaCl concentration of 0.05 mol L^{-1} is employed to control the ionic strength of the sample solution.

The adsorption isotherm of Hb onto the LaMOF-GO_3 composite is carried out by performing the adsorption process at 25 °C within a wide range of initial protein concentration (10−140 mg L^{-1}) in a B-R buffer containing 0.05 mol L^{-1} NaCl at pH 8. As illustrated in Figure S4 (see the Supporting Information), the experimental data fit well with the Langmuir theoretical isotherm model, giving rise to a maximum adsorption capacity of 193 mg g^{-1} for Hb.

The retained protein species on the surface of the LaMOF-GO_3 composite should be recovered by an appropriate elution buffer for further investigations. In accordance with the adsorption profile of Hb on LaMOF-GO_3 within the pH ranges studied, a B-R buffer with higher pH values should be effective for serving as a stripping reagent for Hb desorption. In the present case, B-R buffer at pH 10 is used to recover the adsorbed Hb molecules and the effect of its concentration is investigated, as shown in Figure S5 (see the Supporting

Information). It is clearly observed that a recovery of ca. 63% is achieved at a B-R concentration of 1 mM, whereas the increase in its concentration up to 100 mM results in a decline of the recovery down to 30%. This phenomenon is in accordance with that observed during the adsorption process in the presence of NaCl. When increasing the concentration of the B-R buffer, there are more cationic and anionic species, e.g., PO_4^{3-}, Ac^-, BO_3^{3-}, and Na^+, coexisting in the eluate. In such a case, the higher ionic strength will obviously enhance the interactions between the protein moieties and the sorbent surface, resulting in a decrease of protein recovery. Therefore, a 1 mM B-R buffer at pH 10 is employed for Hb desorption and a recovery of ca. 63% is achieved.

Biocompatibility of LaMOF-GO_3. To confirm the biocompatibility of LaMOF-GO_3 composite, we investigated circular dichroism (CD) spectra of hemoglobin at room temperature on a MOS-450 spectrometer/polarimeter (Bio-logic Science Instrument, France) by using a 0.5 cm quartz cell at 200−500 nm under nitrogen protection. Figure 7 shows the

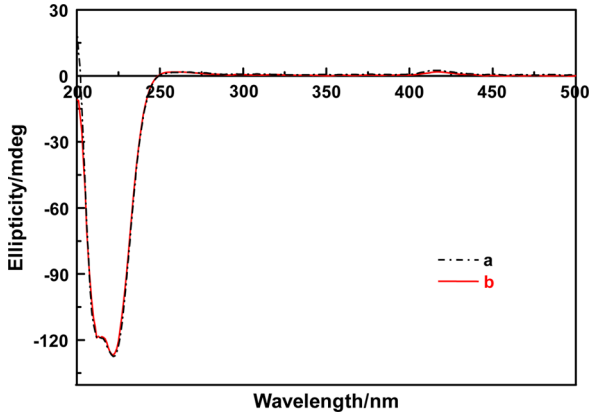

Figure 7. CD spectra of Hb standard solution (150 mg L^{-1}) in 1 mM B-R buffer at pH 10 (dashed line a) and the recovered Hb in the same buffer solution (solid line b).

CD spectra of standard Hb solution (a) and the recovered Hb from the composite (b). Typically, there are two characteristic absorption bands for the original Hb molecules in B-R buffer at pH 10. The stronger one in the UV region contains two negative Cotton peaks at 208 and 222 nm, respectively, which are the typical features of the predominated α-helical structure of protein.[41] The small absorption in the Soret band region (400−420 nm) is related to the characteristic of heme groups in Hb framework.[42] The CD spectrum for the recovered Hb after adsorption/desorption process overlaps completely with that for standard Hb. This demonstrates that there is no obvious change of Hb conformation during the adsorption and desorption processes with LaMOF-GO_3 composite as adsorbent. The favorable biocompatibility of the composite is beneficial for further biological applications.

Selective Isolation of Hemoglobin from Human Whole Blood. The LaMOF-GO_3 composite is employed as adsorbent for the selective isolation of hemoglobin from human whole blood and the collected hemoglobin is further analyzed by SDS-PAGE assay. As seen in Figure 8, there are a few clear protein bands for the human whole blood (Lane 2), which might include serum albumin, hemoglobin, transferin, and immunoglobulin. After adsorption by LaMOF-GO_3 composite, these bands are still clearly observed in the effluent (Lane 3),

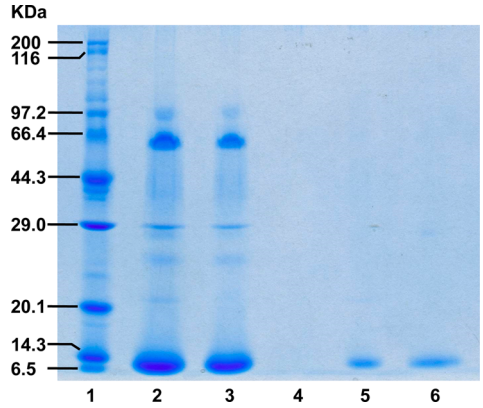

Figure 8. SDS-PAGE assay results. Lane 1, molecular weight standards (Marker in kDa); lane 2, 100-fold diluted human whole blood without pretreatment; lane 3, 100-fold diluted human whole blood after adsorption by LaMOF-GO_3 composite; lane 4, washing solution by deionized water; lane 5, Hb recovered from the LaMOF-GO_3 composite; Lane 6, Hb standard solution of 150 mg L^{-1}.

indicating that no adsorption occurs for them except for hemoglobin. It is seen that no protein bands are observed by washing the composite after adsorption. The stripping by B-R buffer at pH 10 results in a single band for hemoglobin at ca. 6.5 kDa (Lane 5). As a comparison, Lane 6 illustrated the band for 150 mg L^{-1} standard Hb. The SDS-PAGE results indicate that Hb could be selectively isolated from the complex sample matrix, i.e., human whole blood, in the presence of other coexisting proteins of high abundance.

CONCLUSIONS

In this work, graphene oxide-rare earth metal−organic framework composites, LaMOF-GO_n, are prepared through a simple, facile, and large-scale method. GO acts as a template to capture La^{3+} cations and facilitate the crystal growth on its surface. The presence of GO significantly changes the surface morphologies of LaMOF-GO_n composites from spindly rectangular rods to irregular thick blocks with the increase of GO percentage, it also increases the surface area of the composites. The LaMOF-GO_n composites exhibit excellent adsorption properties toward proteins through strong hydrophobic interactions, e.g., $\pi-\pi$ interactions between protein species and the composites. The presence of GO in the structure of LaMOF-GO_n composites facilitates the adsorption of proteins and improves its selectivity toward hemoglobin. In particular, LaMOF-GO_3 composite (at a GO percentage of 3%) shows a favorable selectivity to Hb under controlled conditions, facilitating its selective isolation from the complex sample matrix, namely human whole blood, in the presence of abundant coexisting protein species. In general, the combination of GO and LaMOFs provides a favorable pathway to utilize their unique properties and improve the selective separation performance for proteins. This strategy will broaden the applications of graphene/graphene oxide and metal−organic frameworks in the field of biological separations.

ASSOCIATED CONTENT

Supporting Information

BET surface area, TGA curves, pore size distribution of LaMOFs and LaMOF-GO composite, the effect of ionic strength on Hb adsorption efficiencies, the adsorption isotherm for Hb, and the effect of B-R buffer concentrations on the

recovery of Hb from the LaMOF-GO_3 composite. This material is available free of charge via the Internet at http://pubs.acs.org/.

AUTHOR INFORMATION

Corresponding Authors

*E-mail: chenxuwei@mail.neu.edu.cn. Tel: +86 24 83688944. Fax: +86 24 83676698.

*E-mail: jianhuajrz@mail.neu.edu.cn

Notes

The authors declare no competing financial interest.

ACKNOWLEDGMENTS

This work is financially supported by the Natural Science Foundation of China (21275027, 21235001, and 21375013), the Program of New Century Excellent Talents in University (NCET-11-0071) and Fundamental Research Funds for the Central Universities (N110805001, N120605002, N120405004, and N120605001). The authors also acknowledge Dr. Yide Han for the acquisition of the simulated XRD data of LaMOFs from the single-crystal X-ray diffraction data.

REFERENCES

(1) Zhu, Y. W.; Murali, S.; Cai, W. W.; Li, X. S.; Suk, J. W.; Potts, J. R.; Ruoff, R. S. Graphene and Graphene Oxide: Synthesis, Properties, and Applications. *Adv. Mater.* **2010**, *22*, 3906−3924.

(2) Biswas, C.; Lee, Y. H. Graphene versus Carbon Nanotubes in Electronic Devices. *Adv. Funct. Mater.* **2011**, *21*, 3806−3826.

(3) Dai, L. M. Functionalization of Graphene for Efficient Energy Conversion and Storage. *Acc. Chem. Res.* **2013**, *46*, 31−42.

(4) Jiang, H. J. Chemical Preparation of Graphene-based Nanomaterials and Their Applications in Chemical and Biological Sensors. *Small* **2010**, *7*, 2413−2427.

(5) Wu, S. X.; He, Q. Y.; Tan, C. L.; Wang, Y. D.; Zhang, H. Graphene-Based Electrochemical Sensors. *Small* **2013**, *9*, 1160−1172.

(6) Xiang, Q. J.; Yu, J. G.; Jaroniec, M. Graphene-Based Semiconductor Photocatalysts. *Chem. Soc. Rev.* **2012**, *41*, 782−796.

(7) Li, J. L.; Tang, B.; Yuan, B.; Sun, L.; Wang, X. G. A Review of Optical Imaging and Therapy Using Nanosized Graphene and Graphene Oxide. *Biomaterials* **2013**, *34*, 9519−9534.

(8) Liu, Q.; Shi, J. B.; Sun, J. T.; Wang, T.; Zeng, L. X.; Jiang, G. B. Graphene and Graphene Oxide Sheets Supported on Silica as Versatile and High-Performance Adsorbents for Solid-Phase Extraction. *Angew. Chem., Int. Ed.* **2011**, *50*, 5913−5917.

(9) Liu, J. W.; Zhang, Q.; Chen, X. W.; Wang, J. H. Surface Assembly of Graphene Oxide Nanosheets on SiO_2 Particles for the Selective Isolation of Hemoglobin. *Chem.—Eur. J.* **2011**, *17*, 4864−4870.

(10) Wei, H.; Yang, W. S.; Xi, Q.; Chen, X. Preparation of Fe_3O_4@Graphene Oxide Core-Shell Magnetic Particles for Use in Protein Adsorption. *Mater. Lett.* **2012**, *82*, 224−226.

(11) Liu, J. W.; Yang, T.; Chen, S.; Chen, X. W.; Wang, J. H. Nickel Chelating Functionalization of Graphene Composite for Metal Affinity Membrane Isolation of Lysozyme. *J. Mater. Chem. B* **2013**, *1*, 810−818.

(12) Liu, Q.; Shi, J. B.; Cheng, M. T.; Li, G. L.; Cao, D.; Jiang, G. B. Preparation of Graphene-Encapsulated Magnetic Microspheres for Protein/Peptide Enrichment and MALDI-TOF MS Analysis. *Chem. Commun.* **2012**, *48*, 1874−1876.

(13) Liu, J. W.; Yang, T.; Ma, L. Y.; Chen, X. W.; Wang, J. H. Nickel Nanoparticle Decorated Graphene for Highly Selective Isolation of Polyhistidine-Tagged Proteins. *Nanotechnology* **2013**, *24*, 505704.

(14) Cheng, G.; Wang, Z. G.; Liu, Y. L.; Zhang, J. L.; Sun, D. H.; Ni, J. Z. A Graphene-Based Multifunctional Affinity Probe for Selective Capture and Sequential Identification of Different Biomarkers from Biosamples. *Chem. Commun.* **2012**, *48*, 10240−10242.

(15) Yaghi, O. M.; Keeffe, M. O.; Ockwig, N. W.; Chae, H. K.; Eddaoudi, M.; Kim, J. Reticular Synthesis and the Design of New Materials. *Nature* **2003**, *423*, 705−714.

(16) Meek, S. T.; Greathouse, J. A.; Allendorf, M. D. Metal-Organic Frameworks: a Rapidly Growing Class of Versatile Nanoporous Materials. *Adv. Mater.* **2011**, *23*, 249−267.

(17) Paz, F. A. A.; Klinowski, J.; Vilela, S. M. F.; Tome, J. P. C.; Cavaleiro, J. A. S.; Rocha, J. Ligand Design for Functional Metal-Organic Frameworks. *Chem. Soc. Rev.* **2012**, *41*, 1088−1110.

(18) Gu, Z. Y.; Chen, Y. J.; Jiang, J. Q.; Yan, X. P. Metal-Organic Frameworks for Efficient Enrichment of Peptides with Simultaneous Exclusion of Proteins from Complex Biological Samples. *Chem. Commun.* **2011**, *47*, 4787−4789.

(19) Ma, S. Q.; Zhou, H. C. Gas Storage in Porous Metal-Organic Frameworks for Clean Energy Applications. *Chem. Commun.* **2010**, *46*, 44−53.

(20) Yoon, M.; Srirambalaji, R.; Kim, K. Homochiral Metal-Organic Frameworks for Asymmetric Heterogeneous Catalysis. *Chem. Rev.* **2012**, *112*, 1196−1231.

(21) Achmann, S.; Hagen, G.; Kita, J.; Malkowsky, I. M.; Kiener, C.; Moos, R. Metal-Organic Frameworks for Sensing Applications in the Gas Phase. *Sensors* **2009**, *9*, 1574−1589.

(22) Li, J. R.; Sculley, J.; Zhou, H. C. Metal-Organic Frameworks for Separations. *Chem. Rev.* **2012**, *112*, 869−932.

(23) Gu, Z. Y.; Wang, G.; Yan, X. P. MOF-5 Metal-Organic Framework as Sorbent for In-Field Sampling and Preconcentration in Combination with Thermal Desorption GC/MS for Determination of Atmospheric Formaldehyde. *Anal. Chem.* **2010**, *82*, 1365−1370.

(24) Petit, C.; Bandosz, T. J. MOF-Graphite Oxide Composites: Combing the Uniqueness of Graphene Layers and Metal-Organic Frameworks. *Adv. Mater.* **2009**, *21*, 4753−4757.

(25) Jahan, M.; Bao, Q. L.; Yang, J. X.; Loh, K. P. Structure-Directing Role of Graphene in the Synthesis of Metal-Organic Framework Nanowire. *J. Am. Chem. Soc.* **2010**, *132*, 14487−14495.

(26) Jahan, M.; Liu, Z. L.; Loh, K. P. A Graphene Oxide and Copper-Centered Metal Organic Framework Composite as a Tri-Functional Catalysts for HER, OER and ORR. *Adv. Funct. Mater.* **2013**, *23*, 5363−5372.

(27) Huang, Z. H.; Liu, G. Q.; Kang, F. Y. Glucose-Promoted Zn-Based Metal-Organic Framework/Graphene Oxide Composites for Hydrogen Sulfide Removal. *ACS Appl. Mater. Interfaces* **2012**, *4*, 4942−4947.

(28) Lee, J. H.; Kang, S.; Jaworski, J.; Kwon, K. Y.; Seo, M. L.; Lee, J. Y.; Jung, J. H. Fluorescent Composite Hydrogels of Metal-Organic Frameworks and Functionalized Graphene Oxide. *Chem.—Eur. J.* **2012**, *18*, 765−769.

(29) Hummers, W. S.; Offeman, R. E. Preparation of Graphitic Oxide. *J. Am. Chem. Soc.* **1958**, *80*, 1339−1339.

(30) Kovtyukhova, I.; Olliver, P. J.; Martin, B. R.; Mallouk, T. E.; Chizhik, S. A.; Buzaneva, E. V.; Gorchinskiy, A. D. Layer-by-Layer Assembly of Ultrathin Composite Films from Micro-Sized Graphite Oxide Sheets and Polycations. *Chem. Mater.* **1999**, *11*, 771−778.

(31) Wang, F.; Deng, K. J.; Wu, G. L.; Liao, H. Y.; Liao, H. L.; Zhang, L. L.; Lan, S. M.; Zhang, J. M.; Song, X. G.; Wen, L. L. Facile and Large-Scale Syntheses of Nanocrystal Rare Earth Metal-Organic Frameworks at Room Temperature and Their Photoluminescence Properties. *J. Inorg. Organomet. Polym.* **2012**, *22*, 680−685.

(32) Liu, K.; Zheng, Y. H.; Jia, G.; Yang, M.; Song, Y. H.; Guo, N.; You, H. P. Nano/Micro-Scaled La(1,3,5-BTC)$(H_2O)_6$ Coordination Polymer: Facile Morphology-Controlled Fabrication and Color-Tunable Photoluminescence Properties by co-Doping Eu^{3+}, Tb^{3+}. *J. Solid State Chem.* **2010**, *183*, 2309−2316.

(33) Chen, J. L.; Yan, X. P. A Dehydration and Stabilizer-Free Approach to Production of Stable Water Dispersions of Graphene Nanosheets. *J. Mater. Chem.* **2010**, *20*, 4328−4332.

(34) Paz, F. A. A.; Klinowski, J. Synthesis and Characterization of a Novel Cadmium-Organic Framework with Trimesic Acid and 1,2-Bis(4-pyridyl)ethane. *Inorg. Chem.* **2004**, *43*, 3948−3954.

(35) Wen, Y. H.; Cheng, J. K.; Feng, Y. L.; Zhang, J.; Li, Z. J.; Yao, Y. G. Synthesis of Crystal Structure of $[La(BTC)(H_2O)_6]_n$. *Chin. J. Struct. Chem.* **2005**, *24*, 1440−1444.
(36) Rouquerol, J.; Rouquerol, F.; Sing, K. S. W. In *Adsorption by Powders and Porous Solids: Principles, Methodology and Applications*; Academic Press: San Diego, 1998; Vol. *1*, p 204−205, 427−428, 441.
(37) Hook, F.; Rodahl, M.; Kasemo, B.; Brzezinski, P. Structural Changes in Hemoglobin During Adsorption to Solid Surfaces: Effects of pH, Ionic Strength, and Ligand Binding. *Proc. Natl. Acad. Sci. U.S.A.* **1998**, *95*, 12271−12276.
(38) De, S.; Girigoswami, A. A Fluorimetric and Circular Dichrosim Study of Hemoglobin-Effect of pH and Anionic Amphiphiles. *J. Colloid Interface Sci.* **2006**, *296*, 324−331.
(39) Tsuda, T. In *Electric Field Applications: in Chromatography, Industrial and Chemical Processes.*; Wiley-VCH: New York, 1995; p 35.
(40) Chen, X. W.; Chen, S.; Liu, J. W.; Wang, J. H. Isolation of Hemoglobin from Human Blood Using Solid-Phase Extraction with Lanthanum (III) Modified Zeolite. *Microchim Acta* **2009**, *165*, 217−222.
(41) Guo, X. J.; Han, X. W.; Tong, J.; Guo, C.; Yang, W. F.; Zhu, J. F.; Fu, B. The Investigation of the Interaction between Piracetam and Bovine Serum Albumin by Spectroscopic Methods. *J. Mol. Struct.* **2010**, *966*, 129−135.
(42) Zhu, Y. C.; Cheng, G. J.; Dong, S. J. Structural Electrochemical Study of Hemoglobin by in situ Circular Dichrosim Thin Layer Spectroelectrochemistry. *Biophys. Chem.* **2002**, *97*, 129−138.